Earth **Surface**
Dynamics
Discussions

Clay mineralogy, strontium and neodymium isotope ratios in the sediments of two High Arctic catchments (Svalbard)

Ruth S. Hindshaw[1], Nicholas J. Tosca[2], Alexander M. Piotrowski[1], and Edward T. Tipper[1]

[1]Department of Earth Sciences, University of Cambridge, Downing Street, Cambridge, UK, CB2 3EQ
[2]Department of Earth Sciences, University of Oxford, South Parks Road, Oxford, UK, OX1 3AN

Correspondence to: R. S. Hindshaw (ruth.hindshaw@gmail.com)

Abstract. The identification of sediment sources to the ocean is a pre-requisite to using ocean sediment cores to extract information on past climate and ocean circulation. Sr and Nd isotopes are classical tools with which to trace source provenance. Yet, despite considerable interest in the Arctic Ocean, the circum-Arctic source regions are poorly characterised in terms of their Sr and Nd isotopic compositions. In this study we present Sr and Nd isotope data from the Paleogene Central Basin

5   sediments of Svalbard, including the first published data of river sediments from Svalbard.

The bulk sediments exhibit considerable isotopic variation (εNd_0 = -24.2 to -11.9; $^{87}Sr/^{86}Sr$ = 0.72449 to 0.75243) which can be related to the depositional history of the sediments. In combination with analysis of the clay mineralogy of the sediments, we suggest that the Central Basin sediments were derived from two 'proto' sediment sources. One source is Proterozoic sediments derived from Greenland which are rich in illite and have high $^{87}Sr/^{86}Sr$ and low εNd_0 values. The second source

10 is Carboniferous to Jurassic sediments derived from Siberia which are rich in smectite and have low $^{87}Sr/^{86}Sr$ and high εNd_0 values. Due to a change in deposition conditions throughout the Paleogene (from deep-sea to continental) the relative proportions of these two sources varies in the Central Basin formations. The modern river suspended sediment isotopic composition is then controlled by modern processes, in particular glaciation, which determines the present-day exposure of the formations and therefore the relative contribution of each formation to the suspended sediment load. This study demonstrates that the

15 Sr and Nd isotopic composition of river sediment from the continents exhibits significant seasonal variation, which almost certainly mirrors longer-term hydrological changes, with implications for source provenance studies based on fixed sources through time.

1   Introduction

20 Since the Miocene, the Arctic has been subject to the repeated advance and retreat of ice sheets, a record of which is preserved in ocean sediments (Svendsen et al., 2004; Knies and Gaina, 2008). Thus, the Arctic Ocean and its surrounding seas are a key region for developing our understanding of past ice sheet dynamics and climate. Ocean cores allow us to access the sediment

record and a considerable number of cores have been drilled and analysed in this region (e.g. Vogt et al., 2001; Spielhagen et al., 2004; Knies and Gaina, 2008; Hillaire-Marcel et al., 2013; Fagel et al., 2014; Meinhardt et al., 2016). They provide information on past ocean chemistry through analysis of foraminifera (e.g. Lisiecki and Raymo, 2005), on iceberg abundance through analysis ice-rafted debris (IRD, e.g. Spielhagen et al., 2004) and on past sediment sources through analysis of the

5   mineralogy and geochemistry of the sediment (e.g. France-Lanord et al., 1993).

Clay mineralogy in ocean sediment cores is often used to reconstruct paleoclimate and paleoceanography (e.g. Winkler et al., 2002). However, both the source rock and weathering conditions on the continents affect which clay minerals are formed. For example, kaolinite is more likely to form in tropical climates with intense chemical weathering, whereas illite is more likely to form where physical weathering dominates (Singer, 1984) and the weathering of basalt will likely lead to the formation of

10   smectite, whereas the weathering of granite will likely lead to the formation of illite or kaolinite (Essington, 2004). The Arctic Ocean has a wide variety of source regions ranging from young basalts in Siberia to the Precambrian rocks of Greenland and it is therefore imperative for paleoclimate studies to identify which changes in clay mineralogy are related to a change in climate and which are related to a change in source region.

The radiogenic isotope tracers εNd_0 and $^{87}Sr/^{86}Sr$ are often used together to understand where and how sediment is gener-

15   ated and weathered, enabling source regions to be characterised (Goldstein and Jacobsen, 1988; Cameron and Hattori, 1997; Tricca et al., 1999; Peucker-Ehrenbrink et al., 2010; Lupker et al., 2013; Clinger et al., 2016). εNd_0 is particularly suited to being a source tracer because, unlike Sr and Rb which are fluid mobile, Sm and Nd are immobile and behave very similarly during chemical weathering such that the Sm/Nd ratio does not fractionate during weathering (McCulloch and Wasserburg, 1978) and therefore variations in εNd_0 are predominantly controlled by age (Goldstein and Jacobsen, 1988) rather than the

20   weathering of specific minerals which can affect the Rb-Sr system (e.g. Bullen et al., 1997). Although weathering effects on the neodymium isotopic composition of sediments are considered essentially negligible, it has been shown that in certain circumstances weathering can lead to fractionation of Sm and Nd, leading to variations in εNd_0 in soil profiles (Öhlander et al., 2000; Aubert et al., 2001), which could affect the εNd_0 value of the derived sediments. Variations within soil profiles are either attributed to dust inputs (Viers and Wasserburg, 2004; Ma et al., 2010) and/or the dissolution of accessory phases such

25   as phosphate minerals or Fe-Mn oxyhydroxides (Goldstein and Jacobsen, 1987; Öhlander et al., 2000; Aubert et al., 2001; Babechuk et al., 2015). Additionally, εNd_0 variations in ocean sediments are often interpreted in terms of changing source regions with the isotopic composition of individual source regions remaining constant though time. However, recent studies have hinted at seasonal variations in εNd_0 in river sediments (Viers et al., 2008; Garçon et al., 2013; Lupker et al., 2013), raising the possibility that the εNd_0 value of sediment exported from individual source regions may not remain constant over

30   time. Thus, although εNd_0 is a reliable tracer of source, one region may contain multiple sources, whose relative contributions vary over time.

The source regions to the Arctic Ocean are in general relatively poorly characterised in terms of coupled εNd_0 and $^{87}Sr/^{86}Sr$ measurements with only a few samples from the major rivers and shelf sediments (Eisenhauer et al., 1999; Hillaire-Marcel et al., 2013). Svalbard is particularly important to characterise owing to its location by the Fram Strait, which is the site of

35   deep water formation essential to the functioning of the global thermohaline circulation, and has therefore been the target of

studies seeking to understand the formation of the Atlantic-Arctic gateway (Jakobsson et al., 2007). However, there is neither $^{87}Sr/^{86}Sr$ nor εNd_0 data on river sediments from Svalbard and previous studies aimed at identifying source regions (Tütken et al., 2002; Maccali et al., 2013) have used the bedrock data of granitoids from Ny Friesland in the north-east of Spitsbergen (the largest island in the Svalbard archipelago, Johansson et al., 1995; Johansson and Gee, 1999). Svalbard has a wide range of

5 rocks from different ages and in this study we characterise sediments from the Central Basin (sedimentary formations) which dominates the southern half of Spitsbergen and, being more easily eroded, constitutes a more representative sediment source.

In this study, we provide data characterising sediments from the Central Basin of Svalbard from two catchments and at different times during the melt season. As clay minerals are the main constituent of the rocks in the study area, we combine the geochemical data (εNd_0 and $^{87}Sr/^{86}Sr$) with clay mineralogy in order to identify the factors influencing the unexpectedly

10 large variation in radiogenic isotope compositions observed in the catchment sediments.

2 Field site

Svalbard is located in the Arctic Ocean and has an Arctic climate. In 2012 (the year samples were collected) the mean temperature was -2.0 °C and precipitation was 268 mm, as recorded at Longyearbyen Airport (Nordli et al., 2012). Permafrost is continuous throughout the islands and can be up to 500 m thick (Humlum et al., 2003). Two catchments were studied which

15 are situated adjacent to each other approximately 5 km south of Longyearbyen in central Svalbard.

The first catchment is a permafrost-affected valley called Fardalen (Fig. 1) which is likely to have been unglaciated for at least the last 10 kyr (Svendsen and Mangerud, 1997). The catchment area is 3.4 km² and ranges in elevation from 250 - 1025 m.a.s.l. The second catchment contains a glacier called Dryadbreen and 'Dryadbreen' will be used hereafter to refer to the whole catchment and not just the glacier. Between 1936 and 2006 the area of the glacier decreased from 2.59 to 0.91

20 km² leaving large terminal and lateral ice-cored moraines and a sandur in front of the glacier (Ziaja and Pipała, 2007). The catchment area is 4.8 km² and ranges in elevation from 250 - 1031 m.a.s.l.

2.1 Geological background

The two studied catchments are situated in the Paleogene sedimentary Central Basin of Svalbard. The sedimentary formations exposed in the catchments are from the Van Mijenfjorden group which is Paleocene to Eocene in age (66 - 33.9 Ma) and

25 contains sandstones, siltstones and shale (Fig. 1, Major et al., 2000). The formations exposed in the two catchments have been relatively well studied on account of the fact they cover the Paleocene-Eocene Thermal Maximum (PETM) and formed as a consequence of sedimentation which commenced upon the separation of Greenland from Eurasia (e.g. Helland-Hansen, 1990; Müller and Spielhagen, 1990; Cui et al., 2011; Dypvik et al., 2011; Elling et al., 2016; Jones et al., 2016).

The Central Basin sediments are divided into six formations (Major et al., 2000) which were deposited in a series of

30 transgressive-regressive cycles. The youngest four are exposed in the studied catchments. It is thought that the sediment source for the oldest sediments (mid-Paleocene to early Eocene) was from the east (Carboniferous to Jurassic Siberian basalts, Helland-Hansen, 1990), but this changed to the west (Proterozoic Greenlandic/Canadian High Arctic granites) during early to

mid-Eocene with the erosion of the uplifted West Spitsbergen Fold and Thrust Belt whose formation is linked to rifting of the North Atlantic and the separation of Svalbard from Greenland.

The oldest formations exposed in the studied catchments are the Grumantbyen and Hollendardalen Formations, comprising shallow marine sandstones. The Grumantbyen sediments are part of a regressive trend with sediment derived from the east and

5 possibly the north (Helland-Hansen, 1990). The Hollendardalen sandstones were deposited in the west of the basin from the initial uplift of the fold belt and are coeval with the sediments of the lower Frysajodden Formation.

The youngest three formations comprise a regressive sequence with (from oldest to youngest) the Frysjaodden formation comprising fine-grained shales deposited offshore in an open basin; Battfjellet Formation comprising shallow marine sandstone; and Aspelintoppen comprising continental deposits (Helland-Hansen, 1990; Müller and Spielhagen, 1990). The moun-

10 tain belt is thought to have eroded rapidly (Cui et al., 2011) based on the immaturity of the sandstones (Helland-Hansen, 1990). Detection of pre-Caledonian metamorphic detritus indicates that the mountain belt was eroded down into the basement rocks (Helland-Hansen, 1990). The PETM boundary is near the base of the Frysjaodden Formation (Charles et al., 2011).

3 Methods

A selection of 18 representative rock and sediment samples were sampled from both catchments. The rock samples were

15 first crushed (jaw crusher) and were subsequently ground to fine powders (rotary disc mill and planetary ball mill). For the sediment samples, only the latter step was required. Suspended sediment (>0.2 μm) was also retrieved from nylon filter papers during water sample collection by washing the filter paper with deionized water and then freeze drying the sample. Part of each suspended sediment sample was treated with 5% HCl to remove carbonates. The leachates were not retained. A sub-set of samples were selected for element and isotopic analysis and they are further described here. For all other samples a brief

20 description is included in Table 2. The central part of the unglaciated catchment is dominated by small angular pieces of shale a 1 - 4 cm in length. Samples 'G' and 'R01' are two separate samples of these shale pieces collected from different locations in the unglaciated catchment. In the glaciated catchment transport and physical erosion by glacier has combined rocks from different formations. Samples 'R02' (frost-shattered wacke), 'R03' (litharenite), 'R04' (shale) and 'D' (coarse sediment from glacier surface) were collected from Dryadbreen. Additionally, bank sediment from the stream channels of each catchment

25 were collected (samples 'L' and 'O').

3.1 Semi-quantitative determination of clay mineral abundances

A <2 μm size-fraction was separated from bulk sediments by repeatedly rinsing and re-suspending the sample in de-ionized water with sodium phosphate as a dispersal agent, followed by sonication. The <2 μm fraction was separated by centrifugation (Moore and Reynolds Jr., 1997) and was then transferred to a clean glass slide in preparation for XRD using a filter-peel

30 technique to orientate the sample (Moore and Reynolds Jr., 1997). XRD analysis was performed on a PANalytical PW1050 X-ray diffractometer with a Hiltonbrooks DG2 X-ray generator (Co-Kα radiation) at the University of St. Andrews. Data were collected between 5 and 40° with a step size of 0.02° and a counting time of 3 s per step. Spectra were collected on air-dried,

glycerol-treated, 450°C heated and 550°C heated samples. The glycerol-treated and 450°C spectra were used to obtain semi-quantitative clay mineral abundances using the method outlined in Griffin (1971) which uses the peak heights of kaolinite 001 and illite 001 in the 450°C spectrum and the peak heights of chlorite 004, kaolinite 002, kaolinite 001 and illite 001 in the glycerol treated spectrum to give the relative abundances of kaolinite, chlorite, illite (mica) and expandable layer clay minerals
5   (e.g. smectite and mixed-layer minerals containing smectite).

3.2   Chemical and isotopic composition

A selection of solid samples, separated clay fractions and suspended sediments were analysed for the major and trace element chemistry using the following method: approximately 100 mg of material was ashed at 950°C for 120 minutes. The sample was then digested in a mixture of concentrated hydrofluoric and nitric acids and repeatedly dried down and re-dissolved in 6M
10   HCl. In the final step, the dried down sample was re-dissolved in 2% HNO_3. Major and trace element concentrations were measured at the University of Cambridge by inductively-coupled plasma optical emission spectrometry (ICP-OES, Agilent Technologies 5100) and quadrupole inductively-coupled plasma mass spectrometry (Q-ICP-MS, Perkin Elmer 63 Nexion 350D), respectively.

Neodymium was separated from the matrix using the method described in (Piotrowski et al., 2009). This method uses
15   two columns. The first column contained Eichrom TRUspec resin which separates out REE from the matrix and the second column contains Eichrom LNSpec resin to isolate Nd. The radiogenic neodymium isotopic composition was measured on a Nu plasma (Nu Instruments, University of Cambridge) multi-collector inductively coupled plasma mass spectrometer (MC-ICP-MS). Samples were run at 50-75 ppb with an APEX ACM sample introduction system. Samples were run in triplicate (three measurements on different days) with each measurement comprising 30 cycles with 10 s integration. Samarium interferences
20   were monitored by measuring mass 149. No interferences were detected and oxides were monitored during tuning to ensure they were well below 1% of the beam size. The exponential law was applied to correct for instrument mass fractionation and all $^{143}Nd/^{144}Nd$ ratios were normalised to $^{146}Nd/^{144}Nd = 0.7219$. Standard-sample were bracketing was employed in order to correct for the minor offset with the accepted JNdi-1 value: 0.512060 ± 0.000024 (2SD, n=119) compared with the accepted value of 0.512115 (Tanaka et al., 2000). The USGS shale standard SCo-1 was measured and the $^{143}Nd/^{144}Nd$ value of
25   0.512086 ± 0.000029 (n=3, 2SD) is in agreement with a previously published value of 0.512117 ± 0.000010 (2σ, n=20 Krogstad et al., 2004). In this study, neodymium ratios are reported as deviations relative to the chondritic uniform reservoir (CHUR, $^{143}Nd/^{144}Nd = 0.512638$, Jacobsen and Wasserburg, 1980).

Strontium was separated from the matrix using Biorad mirco bio-spin columns with Eichrom SrSpec resin (Hindshaw, 2011). The radiogenic strontium isotopic compositions were measured on a Neptune MC-ICP-MS (Thermo, University of Cambridge)
30   and were run at 50 ppb using an APEX sample introduction system. Samples were run in triplicate (three measurements on different days) with each measurement comprising 30 cycles with 8 s integration. ^{85}Rb was monitored to correct for rubidium interferences on ^{87}Sr and data were additionally corrected for Kr interferences by measuring ^{83}Kr. The exponential law was applied to correct for instrument mass fractionation and all $^{87}Sr/^{86}Sr$ ratios were normalised to $^{86}Sr/^{88}Sr = 0.1194$. Measure-

ments of NBS 987 gave a $^{87}Sr/^{86}Sr$ value of 0.710249 ± 29 (n=27) and the seawater value was 0.709188 ± 24 (n=9), which is within error of the accepted value of 0.709179 ± 8 (Mokadem et al., 2015).

4 Results

The major and trace element concentrations of the solid samples are provided in Table 1. The measured values are typical for shales (Taylor and McLennan, 1985) and the rare earth element (REE) chondrite normalised element profile of these samples closely follows that of the Post Archaean Australian Shale (PAAS, Table A2). The major element chemistry is very similar to that observed in core samples drilled through the same formations (Fig. 2, Schlegel et al., 2013). Strontium and neodymium concentrations varied from 78 to 139 and 25 to 49 ppm, respectively.

There was a large range in both the strontium and neodymium isotopic compositions of the bulk rocks and sediments: $^{87}Sr/^{86}Sr$ = 0.72449 to 0.75243 and εNd_0 = -24.2 to -11.9. In general, samples collected from Fardalen e.g. R01 and G have higher $^{87}Sr/^{86}Sr$ and lower εNd_0 values than those samples collected in Dryadbreen e.g. D and O (Table 1).

The clay-sized fraction forms a parallel array to the bulk rock samples in εNd_0-$^{87}Sr/^{86}Sr$ space (Fig. 3), with the clay-sized samples having higher εNd_0 and lower $^{87}Sr/^{86}Sr$ values (except for R01). The εNd_0 values of clay fractions were 2.1 to 3.2 epsilon units higher than the corresponding bulk sample and $^{87}Sr/^{86}Sr$ values were 1030 to 2030 ppm lower in the clay compared to the bulk, apart from sample R01 where the clay was 1100 ppm higher in the clay than in the bulk. Rubidium, strontium, neodymium and samarium concentrations are comparable in bulk and clay samples (Table 1) suggesting that clays are the main host of these elements. It has been observed that in a compilation of river sediments from all over the world that εNd_0 in the clay fraction is greater than in the silt-sized fraction by an average of 0.8 epsilon units (Bayon et al., 2015). Fine sediments (as measured by Al/Si ratio) from the Mackenzie River have also been observed to have higher values than coarser sediments (Vonk et al., 2015). The offset in εNd_0 between fine and coarse fractions has been interpreted to reflect the preferential transport of basalt and volcanics in the fine fraction (McLennan et al., 1989; Garçon and Chauvel, 2014; Bayon et al., 2015). A volcanic signal is typically only observed in the first sedimentary cycle, due to the rapid chemical weathering of volcanic particles (McLennan et al., 1989) and therefore, if volcanics are present, they must have been deposited at the same time as the Central Basin sediments. Potential volcanic sources for this period could be the volcanic provinces of North Greenland and Ellesmere Island (58-61 Ma, Jones et al., 2016).

The residues of suspended sediments (collected on 0.2 μm filter paper) after treatment with 5% HCl had higher $^{87}Sr/^{86}Sr$ (3528-4832 ppm) and lower εNd_0 values (1.0 to 4.6 epsilon units) than the corresponding unleached sediment.

4.1 Semi-quantitative clay abundance

Illite, chlorite and kaolinite were present in all the samples analysed. In addition the presence of an expandable layer clay mineral is also evident in the collapse of the XRD signal around 12.7 Å (8 °2θ Co radiation) between the air-dried and glycerol-treated spectra (Fig 4). Additionally, the asymmetry of the illite 001 peak (Fig. 4) suggests that this expandable layer clay mineral is an illite-smectite mixed-layer phase (Moore and Reynolds Jr., 1997) and this is in agreement with the

interpretation by Dypvik et al. (2011) of XRD spectra from core samples from the same formations exposed in the studied catchments. This mixed layer expandable phase will be referred to as 'I/S' in the following discussion. The relative proportions of illite, chlorite, kaolinite and I/S are given in Table 2.

5   The solid samples collected from Dryadbreen tend to have higher illite abundances and lower I/S abundances than those samples collected from Fardalen (Table 2). For all samples, there is an inverse relationship between the relative abundances of I/S and illite (Fig. 4b). The relative abundances of kaolinite and chlorite were similar in both catchments (Table 2). We are not able to distinguish between authigenic and detrital clay minerals.

5 Discussion

5.1 Sediment sources

10   The variation in clay mineralogy, $^{87}Sr/^{86}Sr$ and εNd_0 could be caused by two scenarios: weathering (either modern or in the Eocene) or mixing between two or more sediment sources.

    There are examples from previous studies where chemical weathering has been identified as the cause of an inverse correlation between the relative proportions of illite and smectite (Fig. 5b, e.g. Setti et al., 2004). However, whilst modern day weathering processes can induce large variations in $^{87}Sr/^{86}Sr$ primarily as a result of large inter-mineral variations in the Rb/Sr

15 ratio (e.g. Bullen et al., 1997), it is much harder to induce large variations in the Sm/Nd ratio of minerals and this ratio is often assumed to remain constant once a rock has been formed (e.g. McCulloch and Wasserburg, 1978). Fractionation of the Sm/Nd ratio during chemical weathering has been implicated in the generation of small εNd_0 offsets of around 2 epsilon units (Rickli et al., 2013) and larger variations in εNd_0 were observed in a soil profile developed on granitic till in northern Sweden (Öhlander et al., 2000). In that study a 7.7 epsilon unit variation was observed between the E horizon and the humic horizon,

20 which was attributed to the preferential weathering of minerals enriched in Nd over Sm e.g. allanite. Nevertheless, in the given time period of this study (50 Ma) it is not possible to generate a 14 epsilon unit variation without significant differences in mineralogy where individual minerals have different εNd_0 values. As there is no soil development in the studied catchments, the bulk mineralogy of the samples is broadly similar, as are their Sm/Nd ratios, we rule out chemical weathering as the primary cause of variation. Additionally, the major element chemistry is very similar to that observed in core samples drilled

25 through the same formations (Fig. 2, Schlegel et al., 2013), confirming that weathering processes since the Paleocene have had minor impact on bulk element and, by inference, $^{87}Sr/^{86}Sr$ and εNd_0 values. Therefore, the only way to generate the range of observed range in εNd_0 values is by the mixing of sources with distinct isotope ratios.

    The linear trend between $^{87}Sr/^{86}Sr$ and εNd_0 is suggestive both of a common regional process affecting both isotope systems (Goldstein and Jacobsen, 1988) and of mixing between two end-members. The sediments deposited in the Central Basin

30 during the Eocene were themselves derived from Mesozoic sediments. Based on zircon dating, it is thought that during the Mesozoic, the sediment source to Svalbard alternated between an older (Proterozoic) western component comprised of reworked sediments from Greenland and Canada and a younger (Carboniferous-Jurassic) eastern component from Siberian fold-and-thrust belts (Bue and Andresen, 2014; Elling et al., 2016). The erosion of the Siberian Traps which formed within the same

time period (Permian to Triassic) would also have contributed sediment to the ocean. We will refer to these two sources as 'East' and 'West'.

The Eastern source (Lightfoot et al., 1993; Wooden et al., 1993; Spadea and D'Antonio, 2006) is relatively well-defined since the samples are essentially mono-lithologic (basaltic) and were deposited over a relatively short time-period. Based on zircon

5 dating, both the Uralides and the Verkhoyansk Fold-and-Thrust Belt have been identified as potential sources to Svalbard Mesozoic sediments and the Paleocene Basilika Formation (underlies the Grumantbyen Formation), respectively, (Bue and Andresen, 2014; Elling et al., 2016). The western end-member is much harder to characterise as it consists of Archaean rocks which have undergone extensive metamorphism. We require an end-member with εNd_0 values lower than -24.2 (R03, Table 1) and we therefore only consider data from western Greenland as the East coast was affected by the Caledonian orogeny

10 (Henriksen, 1999) and later by the rifting of the North Atlantic (Bernstein et al., 1998) and therefore has higher (younger) εNd_0 values (Jeandel et al., 2007). The range in $^{87}Sr/^{86}Sr$ and εNd_0 from literature data of Archaean rocks from western and northern Greenland (Jacobsen, 1988; Collerson et al., 1989; Weis et al., 1997; Kalsbeek and Frei, 2006; Friend et al., 2009) is 0.70153 to 2.33356 and -56 to -2.75. By changing the Sr/Nd ratio of these two end-members, mixing lines can be drawn which encompass all the data, with the majority of points falling on a mixing lines with an r value of 1 (i.e. the Sr/Nd ratio of both

15 end-members is the same, Fig. 6).

The variation in clay mineralogy (Fig. 5) can be explained by the different lithological sources of the two end-members (Fig. 6). Basalt typically weathers to smectite group minerals (e.g. Curtin and Smillie, 1981; Parra et al., 1985) and modern sediments originating from Siberia (basaltic) are enriched in smectite (Nürnberg et al., 1994; Wahsner et al., 1999). Any volcanic particles present will also tend to weather to smectite (Bayon et al., 2015). The western source is dominated by granitic rocks where the

20 mica and K-feldspar typically weather to illite and kaolinite, respectively (Essington, 2004). As the western source is older, illite has high Rb/Sr ratios and detrital illite is resistant to weathering, this results in high $^{87}Sr/^{86}Sr$ and low εNd_0. By contrast the younger eastern source will have lower $^{87}Sr/^{86}Sr$ and higher εNd_0 values. These distinct differences between the two sources leads to the observed correlations between clay mineralogy, $^{87}Sr/^{86}Sr$ and εNd_0 values (Fig. 5).

Schlegel et al. (2013) concluded that, on the basis of microscopic observations, the geochemical changes observed between

25 the different formations arose as a result of increased chemical weathering during the late Paleocene and not as a change in source rock provenance, which remained from the west. However, that western source in the Paleocene-Eocene was itself comprised of two sources deposited in the Mesozoic. Chemical weathering during the Paleocene cannot be reconciled with the wide variation in $^{87}Sr/^{86}Sr$ and εNd_0 values. Therefore, the overall trend observed between $^{87}Sr/^{86}Sr$ and εNd_0 is more likely caused by two 'proto-sources' of different ages mixing: an illite-rich end-member with high $^{87}Sr/^{86}Sr$ and low εNd_0 and an

30 illite-poor end-member with low $^{87}Sr/^{86}Sr$ and high εNd_0.

5.2 Difference between catchments

Suspended sediments from the glaciated catchment (Dryadbreen) are distinct from the suspended sediments from the unglaciated catchment (Fardalen) with lower εNd_0, higher $^{87}Sr/^{86}Sr$ values and a greater relative proportion of illite. This is consistent with the rock and sediment samples collected from the two catchments (Tables 1 and 2).

Previously published clay mineralogy and major element data was used to determine which formations the collected rock and sediment samples likely originated from. In a study on the clay-sized fraction of core samples from the Gilsonryggen Member (Riber, 2009; Dypvik et al., 2011), which is a member of the Frysjaodden Formation observed to the south-west of the Central Basin overlying a sandstone wedge (the Hollenderdalen Formation), the relative proportion of illite varied from

5 21-36% and mixed-layer phases were detected, accounting for 17-35% of the clay minerals, in agreement with data from R01 and G (illite 36-46%, I/S 40-50%), suggesting that these samples are from the Frysajodden Formation. The major element chemistry of these two rock samples is also consistent with core data from the Frysjaodden Formation (Schlegel et al., 2013; Hindshaw et al., 2016). Additionally, Schlegel et al. (2013) report the relative proportions of illite, chlorite and smectite in core samples from Aspelintoppen, Battfjellet and Frysjaodden formations. There is a decrease in illite content from 64% in

10 Aspelintoppen to 51% in Frysajodden, suggesting that the samples with a high relative proportion of illite (e.g. D, Table 2) are derived from the Aspelintoppen Formation.

The changes in clay mineralogy between formations are caused by changes in the deposition environment of the Central Basin: from a pro-delta environment (Frysjaodden Formation) to delta progradation (Battfjellet Formation) to finally being filled (Aspelintoppen Formation) (Müller and Spielhagen, 1990; Helland-Hansen, 2010). Sediments are sorted as a function of

15 particle size as they travel through the water, such that coarser particles (typically primary minerals such as feldspar and quartz) will settle faster than finer particles (clay minerals) and within the clay minerals, illite will settle faster than smectite (Sionneau et al., 2008). A size-sorting effect is observed in the difference between the $^{87}Sr/^{86}Sr$ and εNd_0 values of the bulk and the clay-sized fraction. This effect is observed at a global scale and is interpreted to reflect the preferential transport of volcanics and basalt in the fine fraction (Bayon et al., 2015). A similar principle could contribute to the observed array in $^{87}Sr/^{86}Sr$-εNd_0

20 space (Fig. 3). The Frysjaodden Formation, being furthest away from shore, became enriched in smectite-enriched particles derived from the basaltic eastern end-member whereas the Aspelintoppen Formation, deposited in a near-shore environment, became enriched in coarser illite-enriched particles derived from the granitic western end-member. Furthermore, smectite is the only clay mineral which forms in significant amounts in seawater (Griffin et al., 1968) and therefore it is very likely that the deep-sea Frysjaodden Formation contains authigenic smectite in addition to smectite derived from continental weathering,

25 increasing the relative proportion of smectite in this Formation. Taken together, this would suggest that the variation in clay abundances and isotope ratios we observe in the solid samples could reflect the greater relative proportion of the Aspelintoppen Formation relative to the Frysjaodden Formation in rocks and sediments collected in Dyradbreen compared to Fardalen. This would be consistent with the moraine material being predominantly derived from rocks once located in the upper reaches of the catchment (Aspelintoppen Formation) and the modern day sandur plain, containing the products of this physical erosion, is

30 essentially burying the lower down Frysajodden Formation. The difference in the suspended sediments from the two catchments can therefore be explained by a difference in the relative contributions of the formations to the physical erosion products of each catchment. Changes in erosion caused by glaciation could therefore influence the Sr and Nd isotopic of sediments exported to the ocean (von Blanckenburg and Nägler, 2001).

5.3 Effect of leaching

The chemical and isotopic composition of leached suspended sediment is distinct from bulk suspended sediment (Fig. 7a). The residual phase is depleted in MREE (middle rare earth element) and the greater the MREE depletion, the greater the difference in εNd_0 between residue and bulk (Fig. 7b). From mass balance constraints, this points to the existence of a labile pool with

5 low $^{87}Sr/^{86}Sr$ and high εNd_0, which is MREE enriched. There are several possibilities for what the leached phase could be (volcanics, carbonate, apatite) and we will consider each below.

The labile phase could be volcanics. Volcanic ash has a MREE enriched REE pattern (Tepe and Bau, 2014) and would have high εNd_0 and low $^{87}Sr/^{86}Sr$. However, the amount of a volcanic component is expected to be minor in the studied sediments as the volcanic ash component of particulates readily leaches upon contact with seawater (Pearce et al., 2013; Wilson et al.,

10 2013) and therefore may already have been leached during deposition in the Paleocene-Eocene. Additionally, volcanic ash in these layers has been diagenetically altered to bentonites (Cui et al., 2011; Elling et al., 2016; Jones et al., 2016) which are unlikely to be readily leached.

Carbonate minerals would be expected to readily leach in 5% HCl. However, carbonates are unlikely to be the dominant phase leaching because carbonate minerals were only detected in sediments from Dryadbreen (Fig. 4, Hindshaw et al., 2016).

15 The sediments from Dryadbreen would therefore be expected to show the greatest offset between bulk and residue, but in fact it is the sediments from Fardalen, which contain no carbonate, which exhibit the greatest offset between bulk and residue (Fig. 7b). Additionally REE in carbonates are typically LREE enriched relative to chondrite (as are shales) and often have Ce and Eu anomalies (Shaw and Wasserburg, 1985; Schieber, 1988; German and Elderfield, 1990; Komiya et al., 2008; Hua et al., 2013). The residue in Fig. 7b would therefore not be expected to have such a pronounced MREE depletion relative to the bulk, and no

20 obvious Ce or Eu anomalies are observed (Fig. 7b). Finally, carbonate minerals do not typically contain high concentrations of REE (Shaw and Wasserburg, 1985) and it is more likely that other accessory phases, such as apatite, are the main REE carriers.

The REE composition of apatite depends on its origin. Leaching of crystalline apatite leads to a LREE depletion of the residue compared to the bulk in granitic/gneissic catchments (Aubert et al., 2001; Négrel, 2006) and is unlikely to contribute to the leached phase in this study. In contrast, a 'humped' REE pattern in a leachate (i.e. the reverse of Fig. 7b) is characteristic of

25 diagenetically altered apatite (Tricca et al., 1999). Further studies have also linked MREE enrichment in the leached fraction to diagenetic changes associated, not just with phosphates, but also with Fe/Mn oxyhydroxides and clays (Ohr et al., 1994; Johannesson and Zhou, 1999; Su et al., 2017). A diagenetic phase is also consistent with the isotope data where the leached phase is 'younger' (high εNd_0 and low $^{87}Sr/^{86}Sr$) compared to the residue.

The shales in the Frysjaodden Formation were deposited in the marine environment and any authigenic minerals which were

30 formed at that time are likely to have incorporated fluids with the Eocene seawater composition and deep-sea clays are most susceptible to incorporating seawater (Dasch, 1969). This is consistent with the Fardalen sediments, which contain more of the deep-sea Frysjaodden Formation (see previous section), being more affected by leaching than the Dryadbreen sediments (Fig. 7b). In addition to diagenetic changes, adsorption may also occur. Samples containing a greater relative proportion of I/S, have a greater cation exchange capacity and are therefore more likely to contain a greater proportion of ions from seawater,

increasing the difference between $^{87}Sr/^{86}Sr$ and εNd_0 in the residue and bulk (Dasch, 1969; Ohr et al., 1991). The greater difference between εNd_0 in bulk and residue in the Fardalen sediments compared to Dryadbreen is therefore consistent with the greater proportion of I/S in the Fardalen sediments. Adsorption of Nd from seawater was also implicated in a study by von Blanckenburg and Nägler (2001) where leachates of marine sediments had higher εNd_0 than bulk and terrestrial sediments

5   which had had no contact with seawater showed the reverse pattern (lower εNd_0 in leachate compared to bulk).

Assuming the leached phase is comprised of a mixture of authigenic minerals such as apatite and cations readily leached from clay minerals, then the leachate should have a seawater isotopic composition. Radiogenic Sr in seawater in the past is relatively well constrained given that it has a uniform value across the worlds oceans. Radiogenic neodymium, on the other hand, varies between ocean basins. A study based on fish, provides some constraints on the εNd_0 and $^{87}Sr/^{86}Sr$ isotopic composition of

10   the Arctic Ocean during the Eocene (Gleason et al., 2009), with $^{87}Sr/^{86}Sr$ varying from 0.7078 to 0.7088 and εNd_0 varying from -7.5 to -5.5. If we assume that the location of this study and the area of the future Central Basin were connected, then this end-member would be within error of the eastern end-member and therefore could not be distinguished (Fig. 6). This is the most likely reason why the two trends (residue-bulk-leachate and east-west bulk) appear to fall on a common mixing line (Fig. 7a). However, the potential for modification of the main mixing trend set by rock type (Fig. 6) by later diagenetic processes

15   cannot be ruled out and would support the conclusions of Awwiller (1994) who concluded that provenance information based on Nd-Sr isotopes could be obscured by the partial incorporation of Sr and Nd from seawater. Diagenetic alteration has been implicated in shales which give unrealistically old Nd model ages (Arndt and Goldstein, 1987; Awwiller and Mack, 1991; Bock et al., 1994; Cullers et al., 1997; Krogstad et al., 2004).

5.4   Implications for Nd as a sediment source tracer

20   The sediments observed in this study have highly heterogeneous Nd isotopic compositions and the difference in suspended sediment load between the two catchments is up to 6.8 epsilon units. Additionally, seasonal variation is observed: 0.6 epsilon units in Dryabreen and 1.6 epsilon units in Fardalen. A similar magnitude of seasonal variation in εNd_0 has previously been reported in the sediments of much larger rivers. A 1.3 seasonal variation has been reported in suspended sediments from the Madeira River (Amazon, Viers et al., 2008) and a 2 epsilon unit range was observed sediments from two tributaries of the

25   Ganges (Kosi and Narayani, Garçon et al., 2013). The seasonal variation in both of these studies was attributed to the seasonal variation in hydrology which affects how efficient the mixing of tributaries draining different geological units is. The role of hydrology and geology was recently demonstrated at a Canadian glacier where seasonal variations in εNd_0 in a geologically heterogeneous catchment were attributed to the changes in subglacial hydrology (distributed to channelised) which altered where erosion occurred (Clinger et al., 2016). In contrast, glacial catchments with more homogenous lithology have little

30   seasonal variation in εNd_0 (Clinger et al., 2016; Rickli et al., 2017). From this small dataset it would appear that seasonal variations of εNd_0 in suspended sediments are present where rivers drain mixed geology and have a pronounced seasonality to their hydrological cycle.

For the purposes of using Nd in ocean sediment cores as a tracer for past sediment sources it is assumed that the Nd isotopic composition of sediments is constant for broad source regions (e.g. Jeandel et al., 2007), and this will not be affected by sea-

11

sonal variations. However, seasonal cycles give an insight into weathering and erosion conditions under different hydrological regimes that are an analogue for longer term trends. It is entirely plausible that an intensified or weakened hydrological cycle could change the Nd isotopic composition of sediment export for a given region. Of particular relevance to the Arctic region is the re-organisation of drainage basins as the ice sheets waxed and waned and the attendant changes in magnitude and location of discharge to the ocean (e.g. Teller, 1990; Wickert, 2016). Therefore, it should not necessarily be assumed that the continental regions have had a constant εNd_0 export to the oceans. For example, the 5.7 epsilon unit range in εNd_0 (which is of similar magnitude to difference between catchments observed in this study) in an Arctic sediment core (PS1533, Tütken et al., 2002) over the last 140 ka was attributed to changes in the relative proportion of sediment derived from two isotopically distinct sources (Svalbard and Siberia) over glacial-interglacial cycles. Although the broad end-member identification will unlikely be affected, the calculated proportions of each end-member at different points in time would change if the those end-members are not constant over glacial-interglacial cycles.

6 Conclusions

The large variations in $^{87}Sr/^{86}Sr$ and εNd_0 observed in two small catchments in Svalbard can be explained as a result of two isotopically and geochemically distinct 'proto-sources' mixing during the Meoszoic and subsequently forming the Paleocene-Eocene sedimentary formations which are eroding today (Fig. 8). The two original sources are an eastern source derived from basaltic rocks from Siberia and a western source derived from granitic rocks from Greenland. The original geology of the sources controls the initial geochemistry, Sr and Nd isotope values and subsequently determines the type of clay minerals formed during weathering, susceptibility to later diagenesis and particle-size transport effects.

Changes in erosion caused by the glaciation of Dryadbreen has led to material from the upper (younger) formation, which contains a higher proportion of material derived from the western source, being moved lower down in the catchment where it is present in the moraines. In contrast, the lower (older) formation, which contains a higher proportion of material derived from the eastern source, is fully exposed in the unglaciated catchment, having not been covered by sediment from the upper reaches of the catchment. This leads to a marked difference in the suspended sediment export from the two catchments and suggests that changes in continental erosion during glacial-interglacial cycles could have a pronounced effect on the Sr and Nd isotopic composition of sediment exported from sedimentary catchments where those sediments have a complex history of multiple sources and sedimentary cycles. Given that the majority of the main rivers in the circum-Arctic region drain shale, the temporal variation of $^{87}Sr/^{86}Sr$ and εNd_0 exported to the ocean from this region over glacial-interglacial periods, may not have been constant. Further changes on the continents occurring during glacial-interglacial cycles (hydrology, basin configuration) should also be considered as factors affecting εNd_0 variation in ocean sediments.

Data availability. All data used in this manuscript is contained in the included tables apart from XRD data files. For data related queries, please contact the corresponding author.

Competing interests. The authors declare no competing interests.

References

Arndt, N. T. and Goldstein, S. L.: Use and abuse of crust-formation ages, Geology, 15, 893–895, 1987.

Aubert, D., Stille, P., and Probst, A.: REE fractionation during granite weathering and removal by waters and suspended loads: Sr and Nd isotopic evidence, Geochim. Cosmochim. Acta, 65, 387–406, 2001.

5 Awwiller, D. N.: Geochronology and mass transfer in Gulf Coast mudrocks (south-central Texas, U.S.A.): Rb-Sr, Sm-Nd and REE systematics, Chem. Geol., 116, 61–84, 1994.

Awwiller, D. N. and Mack, L. E.: Diagenetic modification of Sm-Nd model ages in Tertiary sandstones and shales, Texas Gulf Coast, Geology, 19, 311–314, 1991.

Babechuk, M. G., Widdowson, M., Murphy, M., and Kamber, B. S.: A combined Y/Ho, high field strength element (HFSE) and Nd isotope

10 perspective on basalt weathering, Deccan Traps, India, Chem. Geol., 369, 25–41, 2015.

Bayon, G., Toucanne, S., Skonieczny, C., André, L., Bermell, S., Cheron, S., Dennielou, B., Etoubleau, J., Freslon, N., Gauchery, T., Germain, Y., Jorry, S. J., Ménot, G., Monin, L., Pnzevera, E., Rouget, M. L., Tachikawa, K., and Barrat, J. A.: Rare earth elements and neodymium isotopes in world river sediments revisited, Geochim. Cosmochim. Acta, 170, 17–38, https://doi.org/10.1016/j.gca.2015.08.001, 2015.

Bernstein, S., Kelemen, P. B., Tegner, C., Kurz, M. D., Blusztajn, J., and Brooks, C. K.: Post-breakup basaltic magmatism along the East

15 Greenland Tertiary rifted margin, Earth Planet. Sci. Lett., 160, 845–862, 1998.

Bock, B., McLennan, S. M., and Hanson, G. N.: Rare earth element redistribution and its effects on the neodymium isotope system in the Austin Glen Member of the Normanskill Formation, New York, USA, Geochim. Cosmochim. Acta, 58, 5245–5253, 1994.

Bue, E. P. and Andresen, A.: Constraining depositional models in the Barents Sea region using detrital zircon U-Pb data from Mesozoic sediments in Svalbard, in: Sediment provenance studies in hydrocarbon exploration and production, edited by Scott, R. A., Smyth, H. R.,

20 Morton, A. C., and Richardson, N., no. 386 in Special Publications, pp. 261–279, Geological Society, 2014.

Bullen, T., White, A., Blum, A., Harden, J., and Schulz, M.: Chemical weathering of a soil chronosequence on granitoid alluvium: II. Mineralogic and isotopic constraints on the behavior of strontium, Geochim. Cosmochim. Acta, 61, 291–306, 1997.

Cameron, E. M. and Hattori, K.: Strontium and neodymium isotope ratios in the Fraser River, British Columbia: a riverine transect across the Cordilleran orogen, Chem. Geol., 137, 243–253, 1997.

25 Charles, A. J., Condon, D. J., Harding, I. C., Pälike, H., Marshall, A. T., Cui, Y., Kump, L., and Croudace, I. W.: Constraints on the numerical age of the Paleocene-Eocene boundary, Geochem. Geophys. Geosys., 12, Q0AA17, https://doi.org/10.1029/2010GC003426, 2011.

Clinger, A. E., Aciego, S. M., Stevenson, E. I., Arendt, C. A., and Robbins, M. J.: Implications for post-comminution processes in subglacial suspended sediment using coupled radiogenic strontium and neodymium isotopes, Geomorphology, 259, 134–144, https://doi.org/10.1016/j.geomorph.2016.02.006, 2016.

30 Collerson, K. D., McCulloch, M. T., and Nutman, A. P.: Sr and Nd isotope systematics of polymetamorphic Archean gneisses from souther West Greenland and northern Labrador, Can J. Earth Sci., 26, 446–466, 1989.

Cui, Y., Kump, L. R., Ridgwell, A. J., Charles, A. J., Junium, C. K., Diefendorf, A. F., Freeman, K. H., Urban, N. M., and Harding, I. C.: Slow release of fossil carbon during the Palaeocene–Eocene Thermal Maximum, Nat. Geosci., 4, 481–485, 2011.

Cullers, R. L., Bock, B., and Guidotti, C.: Elemental distributions and neodymium isotopic compositions of Silurian metasediments, western

35 Maine, USA: Redistribution of the rare earth elements, Geochim. Cosmochim. Acta, 61, 1847–1861, 1997.

Curtin, D. and Smillie, G. W.: Composition and origin of smectite in soils derived from basalt in Northern Ireland, Clay Clay Miner., 29, 277–284, 1981.

Dasch, E. J.: Strontium isotopes in weathering profiles, deep-sea sediments, and sedimentary rocks, Geochim. Cosmochim. Acta, 33, 1521–1552, 1969.

Dypvik, H., Riber, L., Burca, F., Rüther, D., Jargvoll, D., Nagy, J., and Jochmann, M.: The Paleocene-Eocene thermal maximum (PETM) in Svalbard - clay mineral and geochemical signals, Palaeogeogr. Palaeoclimatol. Palaeoecol., 302, 156–169, 2011.

5 Eisenhauer, A., Meyer, H., Rachold, V., Tütken, T., Wiegand, B., Hansen, B. T., Spielhagen, R. F., Lindemann, F., and Kassens, H.: Grain size separation and sediment mixing in Arctic Ocean sediments: evidence from the strontium isotope systematic, Chem. Geol., 158, 173–188, 1999.

Elling, F. J., Spiegel, C., Estrada, S., Davis, D. W., Reinhardt, L., Henjes-Kunst, F., Allroggen, N., Dohrmann, R., Piepjohn, K., and Lisker, F.: Origin of bentonites and detrital zircons of the Paleocene Basilika Formation, Svalbard, Front. Earth Sci., 4, 73,
10 https://doi.org/10.3389/feart.2016.00073, 2016.

Essington, M. E.: Soil and Water Chemistry: An Integrative Approach, CRC Press, 2004.

Fagel, N., Not, C., Gueibe, J., Mattielli, N., and Bazhenova, E.: Late Quaternary evolution of sediment provenances in the Central Arctic Ocean: mineral assemblage, trace element composition and Nd and Pb isotope fingerprints of detrital fraction from the Northern Mendeleev Ridge, Quaternary Sci. Rev., 92, 140–154, 2014.

15 France-Lanord, C., Derry, L., and Michard, A.: Evolution of the Himalaya since Miocene time: isotopic and sedimentological evidence from the Bengal Fan, in: Himalayan Tectonics, edited by Treloar, P. J. and Searle, M. P., 74, pp. 603–621, Geological Society Speical Publication, 1993.

Friend, C. R. L., Nutman, A. P., Baadsgaard, H., and Duke, M. J. M.: The whole rock Sm-Nd 'age' for the 2825 Ma Ikkattoq gneisses (Greenland) is 800 Ma too young: Insights into Archaean TTG petrogenesis, Chem. Geol., 261, 62–76, 2009.

20 Garçon, M. and Chauvel, C.: Where is basalt in river sediments, and why does it matter?, Earth Planet. Sci. Lett., 407, 61–69, 2014.

Garçon, M., Chauvel, C., France-Lanord, C., Huyghe, P., and Lavé, J.: Continental sedimentary processes decouple Nd and Hf isotopes, Geochim. Cosmochim. Acta, 121, 177–195, 2013.

German, C. R. and Elderfield, H.: Application of the Ce anomaly as a paleoredox indicator: the ground rules, Paleoceanography, 5, 823–833, 1990.

25 Gleason, J. D., Thomas, D. J., Moore Jr., T. C., Blum, J. D., Owen, R. M., and Haley, B. A.: Early to middle Eocene history of the Arctic Ocean from Nd-Sr isotopes in fossil fish debris, Lomonosov Ridge, Paleoceanography, 24, PA2215, https://doi.org/10.1029/2008PA001685, 2009.

Goldstein, S. L. and Jacobsen, S. B.: The Nd and Sr isotopic systematics of river-water dissolved material: implications for the sources of Nd and Sr in seawater, Chem. Geol., 66, 245–272, 1987.

30 Goldstein, S. L. and Jacobsen, S. B.: Nd and Sr isotopic systematics of river water suspended material: implications for crustal evolution, Earth Planet. Sci. Lett., 87, 249–265, 1988.

Griffin, G. M.: Interpretation of X-ray diffraction data, in: Procedures in sedimentary petrology, edited by Carver, R. E., pp. 541–569, Wiley-Interscience, New York, 1971.

Griffin, J. J., Windom, H., and Goldberg, E. D.: The distribution of clay minerals in the World Ocean, Deep-Sea Res., 15, 433–459, 1968.

35 Helland-Hansen, W.: Sedimentation in Paleogene Foreland Basin, Spitsbergen, AAPG Bull., 74, 260–272, 1990.

Helland-Hansen, W.: Facies and stacking patterns of shelf-deltas within the Palaeogene Battfjellet Formation, Nordenskiöld Land, Svalbard: implications for subsurface reservoir prediction, Sedimentology, 57, 190–208, https://doi.org/10.1111/j.1365-3091.2009.01102.x, 2010.

Henriksen, N.: Conclusion of the 1:500 000 mapping project in the Caledonian fold belt in North-East Greenland, in: Review of Greenland activities 1998, edited by Higgins, A. K. and Watt, W. S., vol. 183 of *Geology of Greenland Survey Bulletin*, pp. 10–22, GEUS, 1999.

Hillaire-Marcel, C., Maccali, J., Not, C., and Poirier, A.: Geochemical and isotopic tracers of Arctic sea ice sources and export with special attention to the Younger Dryas interval, Quaternary Sci. Rev., 79, 184–190, 2013.

5 Hindshaw, R. S.: Chemical weathering and calcium isotope fractionation in a glaciated catchment, Ph.D. thesis, ETH Zurich, 2011.

Hindshaw, R. S., Heaton, T. H. E., Boyd, E. S., Lindsay, M. R., and Tipper, E. T.: Influence of glaciation on mechanisms of mineral weathering in two high Arctic catchments, Chem. Geol., 420, 37–50, https://doi.org/10.1016/j.chemgeo.2015.11.004, 2016.

Hua, G., Yuansheng, D., Lian, Z., Jianghai, Y., and Hu, H.: Trace and rare earth elemental geochemistry of carbonate succession in the Middle Gaoyuzhuang Formation, Pingquan section: Implications for early Mesoproterozoic ocean redox conditions, J. Palaeogeogr., 2,

10 209–221, 2013.

Humlum, O., Instanes, A., and Sollid, J. L.: Permafrost in Svalbard: a review of research history, climatic background and engineering challenges, Polar Res., 22, 191–215, https://doi.org/10.3402/polar.v22i2.6455, 2003.

Jacobsen, S. B.: Isotopic constraints on crustal growth and recycling, Earth Planet. Sci. Lett., 90, 315–329, 1988.

Jacobsen, S. B. and Wasserburg, G. J.: Sm-Nd isotopic evolution of chondrites, Earth Planet. Sci. Lett., 50, 139–155, 1980.

15 Jakobsson, M., Backman, J., Rudels, B., Nycander, J., Frank, M., Mayer, L., Jokat, W., Sangiorgi, F., O'Regan, M., Brinkhuis, H., King, J., and Moran, K.: The early Miocene onset of a ventilated circulation regime in the Arctic Ocean, Nature, 447, 986–990, 2007.

Jeandel, C., Arsouze, T., Lacan, F., Téchiné, P., and Dutay, J.-C.: Isotopic Nd compositions and concentrations of the lithogenic inputs into the ocean: a compilation, with an emphasis on the margins, Chem. Geol., 239, 156–164, 2007.

Johannesson, K. H. and Zhou, X.: Origin of middle rare earth element enrichments in acid waters of a Canadian High Arctic Lake, Geochim.

20 Cosmochim. Acta, 63, 153–165, 1999.

Johansson, Å. and Gee, D. G.: The late Palaeoproterozoic Eskolabreen granitoids of southern Ny Friesland, Svalbard Caledonides - geochemistry, age, and origin, GFF, 121, 113–126, 1999.

Johansson, Å., Gee, D. G., Björklund, L., and Witt-Nilsson, P.: Isotope studies of granitoids from the Bangenhuk Formation, Ny Friesland Caledonides, Svalbard, Geol. Mag., 132, 303–320, 1995.

25 Jones, M. T., Eliassen, G. T., Shephard, G. E., Svensen, H. H., Jochmann, M., Friis, B., Augland, L. E., Jerram, D. A., and Planke, S.: Provenance of bentonite layers in the Paleocene strata of the Central Basin, Svalbard: implications for magmatism and rifting events around the onset of the North Atlantic Igneous Province, J. Volcan. Geo. Res., 327, 571–584, 2016.

Kalsbeek, F. and Frei, R.: The Mesoproterozoic Midsommersø dolerites and associated high-silica intrusions, North Greenland: crustal melting, contamination and hydrothermal alteration, Contrib. Mineral. Petrol., 152, 89–110, 2006.

30 Knies, J. and Gaina, C.: Middle Miocene ice sheet expansion in the Arctic: Views from the Barents Sea, Geochem. Geophys. Geosyst., 9, Q02 015, 2008.

Komiya, T., Hirata, T., Kitajima, K., Yamamoto, S., Shibuya, T., Sawaki, Y., Ishikawa, T., Shu, D., Li, Y., and Han, J.: Evolution of the composition of seawater through geologic time, and its influence on the evolution of life, Godwana Res., 14, 159–174, 2008.

Krogstad, E. J., Fedo, C. M., and Eriksson, K. A.: Provenance ages and alteration histories of shales from the Middle Archean Buhwa

35 greenstone belt, Zimbabwe: Nd and Pb isotopic evidence, Geochim. Cosmochim. Acta, 68, 319–332, 2004.

Lightfoot, P. C., Hawkesworth, C. J., Hergt, J., Naldrett, A. J., Gorbachev, N. S., Fedorenko, V. A., and Doherty, W.: Remobilidation of the continental lithosphere by a mantle plume: major-, trace-element, and Sr-, Nd-, and Pb-isotope evidence from picritic and thloeiitic lavas of the Noril'sk District, Siberian Trap, Russia, Contrib. Mineral. Petrol., 114, 171–188, 1993.

Lisiecki, L. E. and Raymo, M. E.: A Pliocene-Pleistocene stack of 57 globally distributed benthic δ^{18}O records, Paleoceanography, 20, PA1003, https://doi.org/10.1029/2004PA001071, 2005.

Lupker, M., France-Lanord, C., Galy, A., Lavé, J., and Kudrass, H.: Increasing chemical weathering in the Himalayan streams since the Last Glacial Maximum, Earth Planet. Sci. Lett., 365, 243–252, 2013.

5   Ma, J., Wei, G., Xu, Y., and Long, W.: Variations of Sr-Nd-Hf isotopic systematics in basalt during intensive weathering, Chem. Geol., 269, 376–385, 2010.

Maccali, J., Hillaire-Marcel, C., Carignan, J., and Reisberg, L. C.: Geochemical signatures of sediments documenting Arctic sea-ice and water mass export through Fram Strait since the Last Glacial Maximum, Quaternary Sci. Rev., 64, 136–151, https://doi.org/10.1016/j.quascirev.2012.10.029, 2013.

10   Major, H., Haremo, P., Dallmann, W. K., and Andresen, A.: Geological map of Svalbard 1:100 000, sheet C9G Adventdalen, Temakart nr. 31, Norsk Polarinstitutt, Tromsø, Norway, 2000.

McCulloch, M. T. and Wasserburg, G. J.: Sm-Nd and Rb-Sr chronology of continental crust formation, Science, 200, 1003–1011, 1978.

McLennan, S. M., McCulloch, M. T., Taylor, S. R., and Maynard, J. B.: Effects of sedimentary sorting on neodymium isotopes in deep-sea turbidites, Nature, 337, 547–549, 1989.

15   Meinhardt, A.-K., Pahnke, K., Böning, B., and Brumsack, H.-J.: Climate change and response in bottom water circulation and sediment provenance in the Central Arctic Ocean since the Last Glacial, Chem. Geol., 427, 98–108, 2016.

Mokadem, F., Parkinson, I. J., Hathorne, E. C., Anand, P., Allen, J. T., and Burton, K. W.: High-precision radiogenic strontium isotope measurements of the modern and glacial ocean: Limits on glacial-interglacial variations in continental weathering, Earth Planet. Sci. Lett., 415, 111–120, https://doi.org/10.1016/j.epsl.2015.01.036, 2015.

20   Moore, D. M. and Reynolds Jr., R. C.: X-ray diffraction and the identification and analysis of clay minerals, Oxford University Press, New York, 1997.

Müller, R. D. and Spielhagen, R. F.: Evolution of the Central Tertiary Basin of Spitsbergen: towards a synthesis of sediment and plate tectonic history, Palaeogeogr. Palaeoclimatol. Palaeoecol., 80, 153–172, 1990.

Négrel, P.: Water-granite interaction: Clues from strontium, neodymium and rare-earth elements in soil and waters, Appl. Geochem., 21, 25   1432–1454, 2006.

Nordli, Ø., Przybylak, R., Ogilvie, A. E. J., and Isaksen, K.: Long-term temperature trends and variability on Spitsbergen: the extended Svalbard Airport temperature series, 1898-2012, Polar Res., 33, 21 349, https://doi.org/10.3402/polar.v33.21349, 2012.

Nürnberg, D., Wollenburg, I., Dethleff, D., Eicken, H., Kassens, H., Letzig, T., Reimnitz, E., and Thiede, J.: Sediments in Arctic sea ice: implications for entrainment, transport and release, Marine Geology, 119, 185–214, 1994.

30   Öhlander, B., Ingri, J., Land, M., and Schöberg, H.: Change of Sm-Nd isotope composition during weathering of till, Geochim. Cosmochim. Acta, 64, 813–820, 2000.

Ohr, M., Halliday, A. N., and Peacor, D. R.: Sr and Nd isotopic evidence for punctuated clay diagenesis, Texas Gulf Coast, Earth Planet. Sci. Lett., 105, 110–126, 1991.

Ohr, M., Halliday, A. N., and Peacor, D. R.: Mobility and fractionation of rare earth elements in argillaceous sediments: Implications for 35   dating diagenesis and low-grade metamorphism, Geochim. Cosmochim. Acta, 58, 289–312, 1994.

Parra, M., Delmont, P., Ferragne, A., Latouche, C., Pons, J. C., and Puechmaille, C.: Origin and evolution of smectites in recent marine sediments of the NE Atlantic, Clay Miner., 20, 335–346, 1985.

Pearce, C. R., Jones, M. T., Oelkers, E. H., Pradoux, C., and Jeandel, C.: The effect of particulate dissolution on the neodymium Nd isotope and Rare Earth Element (REE) composition of seawater, Earth Planet. Sci. Lett., 369-370, 138–147, 2013.

Peucker-Ehrenbrink, B., Miller, M. W., Arsouze, T., and Jeandel, C.: Continental bedrock and riverine fluxes of strontium and neodymium isotopes to the oceans, Geochem. Geophys. Geosys., 11, Q03 016, https://doi.org/10.1029/2009GC002869, 2010.

5 Piotrowski, A. M., Banakar, V. K., Scrivner, A. E., Elderfield, H., Galy, A., and Dennis, A.: Indian Ocean circulation and productivity during the last glacial cycle, Earth Planet. Sci. Lett., 285, 179–189, 2009.

Riber, L.: Paleogene depositional conditions and climatic changes of the Frysjaodden Formation in central Spitsbergen (sedimentology and mineralogy), Master's thesis, University of Oslo, 2009.

Rickli, J., Frank, M., Stichel, T., Georg, R. B., Vance, D., and Halliday, A. N.: Controls on the incongruent release of hafnium during
10   weathering of metamorphic and sedimentary catchments, Geochim. Cosmochim. Acta, 101, 263–284, 2013.

Rickli, J., Hindshaw, R. S., Leuthold, J., Wadham, J. L., Burton, K. W., and Vance, D.: Impact of glacial activity on the weathering of Hf isotopes - observations from Southwest Greenland, Geochim. Cosmochim. Acta, 2017.

Schieber, J.: Redistribution of rare-earth elements during diagenesis of carbonate rocks from the mid-Proterozoic Newland Formation, Montana, U.S.A., Chem. Geol., 69, 111–126, 1988.

15 Schlegel, A., Lisker, F., Dörr, N., Jochmann, M., Schubert, K., and Spiegel, C.: Petrography and geochemistry of siliclastic rocks from the Central Tertiary Basin of Svalbard - implications for provenance, tectonic setting and climate, Z. Dt. Ges. Geowiss., 164, 173–186, 2013.

Setti, M., Marinoni, L., and López-Galindo, A.: Mineralogic and geochemical characteristics (major, minor, trace elements and REE) of detrital and authigenic clay minerals in a Cenozoic sequence from Ross Sea, Antarctica, Clay Miner., 39, 405–421, https://doi.org/10.1180/000985503540143, 2004.

20 Shaw, H. F. and Wasserburg, G. J.: Sm-Nd in marine carbonates and phosphates: Implications for Nd isotopes in seawater and crustal ages, Geochim. Cosmochim. Acta, 49, 503–518, 1985.

Singer, A.: The paleoclimatic interpretation of clay minerals in sediments - a review, Earth Sci. Rev., 21, 251–293, 1984.

Sionneau, T., Bout-Roumateilles, V., Biscaye, P. E., Van Vliet-Lanoe, B., and Bory, A.: Clay mineral distributions in and around the Mississippi River watershed and Northern Gulf of Mexico: sources and transport patterns, Quaternary Sci. Rev., 27, 1740–1751, 2008.

25 Spadea, P. and D'Antonio, M.: Initiation and evolution of intra-oceanic subduction in the Uralides: Geochemical and isotopic constraints from Devonian oceanic rocks of the Southern Urals, Russia, Island Arc, 15, 7–25, 2006.

Spielhagen, R. F., Baumann, K.-H., Erlenkeuser, H., Nowaczyk, R., Nørgaard-Pedersen, N., Vogt, C., and Weiel, D.: Arctic ocean deep-sea record of northern Eurasian ice sheet history, Quaternary Sci. Rev., 23, 1455–1483, 2004.

Su, N., Yang, S., Guo, Y., Yue, W., Wang, X., Yin, P., and Huang, X.: Revisit of rare earth element fractionation during chemical weathering
30   and river sediment transport, Geochem. Geophys. Geosys., 18, 935–955, https://doi.org/10.1002/2016GC006659, 2017.

Svendsen, J. I. and Mangerud, J.: Holocene glacial and climatic variations on Spitsbergen, Svalbard, Holocene, 7, 45–57, https://doi.org/10.1177/095968369700700105, 1997.

Svendsen, J. I., Alexanderson, H., Astakhov, V. I., Demidov, I., Dowdeswell, J. A., Funder, S., Gataullin, V., Henriksen, M., Hjort, C., Houmark-Nielsen, M., Hubberten, H. W., Ingólfsson, O., Jakobsson, M., Kjær, K. H., Larsen, E., Lokrantz, H., Lunkka, J. P., Lsyå, A.,
35   Mangerud, J., Matiouchkov, A., Murray, A., Möller, P., Niessen, F., Nikolyskaya, O., Polyak, L., Saarnisto, M., Siegert, S., Siegert, M. J., Spielhagen, R. F., and Stein, R.: Late Quternary ice sheet history of northern Eurasia, Quaternary Sci. Rev., 23, 1229–1271, 2004.

Tanaka, T., Togashi, S., Kamioka, H., Amakawa, H., Kagami, H., Hamamoto, T., Yuhara, M., Orihashi, Y., Yoneda, S., Shimizu, H., Ku-
nimaru, T., Takahashi, K., Yanagi, T., Nakano, T., Fujimaki, H., Shinjo, R., Asahara, Y., Tanimizu, M., and Dragusanu, C.: JNd-1: a
neodymium isotopic reference in consistency with LaJolla neodymium, Chem. Geol., 168, 279–281, 2000.

Taylor, S. R. and McLennan, S. M.: The continental crust: Its composition and evolution, Blackwell Scientific, Boston, Mass., 1985.

5 Teller, J. T.: Volume and routing of late-glacial runoff from the southern Laurentide ice Sheet, Quaternary Res., 34, 12–23, 1990.

Tepe, N. and Bau, M.: Importance of nanoparticles and colloids from volcanic ash for riverine transport of trace elements to the ocean:
Evidence from glacial-fed rivers after the 2010 eruption of Eyjafjallajökull Volcano, Iceland, Sci. Tot. Environ., 488-489, 243–251, 2014.

Tricca, A., Stille, P., Steinmann, M., Kiefel, B., Samuel, J., and Eikenberg, J.: Rare earth elements and Sr and Nd isotopic compositions of
dissolved and suspended loads from small river systems in the Vosges mountains (France), the river Rhine and groundwater, Chem. Geol.,
10 160, 139–158, 1999.

Tütken, T., Eisenhauer, A., Wiegand, B., and Hansen, B. T.: Glacial-interglacial cycles in Sr and Nd isotopic composition of Arctic marine
sediments triggered by the Svalbard/Barents Sea ice sheet, Marine Geology, 182, 351–372, 2002.

Viers, J. and Wasserburg, G. J.: Behavior of Sm and Nd in a lateritic soil profile, Geochim. Cosmochim. Acta, 68, 2043–2054,
https://doi.org/10.1016/j.gca.2003.10.034, 2004.

15 Viers, J., Roddaz, M., Filizola, N., Guyot, J.-L., Sondag, F., Brunet, P., Zouiten, C., Boucayrand, C., Martin, F., and Boaventura, G. R.:
Seasonal and provenance controls on Nd-Sr isotopic compositions of Amazon rivers suspended sediments and implications for Nd and Sr
fluxes to the Atlantic Ocean, Earth Planet. Sci. Lett., 274, 511–523, 2008.

Vogt, C., Knies, J., Spielhagen, R. F., and Stein, R.: Detailed mineralogical evidence for two nearly identical glacial/interglacial cycles and
Atlantic water advection to the Arctic Ocean during the last 90,000 years, Global Planet. Change, 31, 23–44, 2001.

20 von Blanckenburg, F. and Nägler, T. F.: Weathering versus circulation-controlled changes in radiogenic isotope tracer composition of the
Labrador Sea and North Atlantic Deep Water, Paleoceanography, 16, 424–434, 2001.

Vonk, J. E., Giosan, L., Blusztajn, J., Montlucon, D., Pannatier, E. G., McIntyre, C., Wacker, L., Macdonald, R. W., Yunker, M. B., and Eglin-
ton, T. I.: Spatial variations in geochemical characteristics of the modern Mackenzie Delta sedimentary system, Geochim. Cosmochim.
Acta, 171, 100–120, 2015.

25 Wahsner, M., Müller, C., Stein, R., Ivanov, G., Levitan, M., Shelekhova, E., and Tarasov, G.: Clay-mineral distribution in surface sediments of
the Eurasian Arctic Ocean and continental margin as indicator for source areas and transport pathways - a synthesis, Boreas, 28, 215–232,
1999.

Weis, D., Demaiffe, D., Souchez, R., Gow, A. J., and Meese, D. A.: Ice sheet development in Central Greenland: implications from the Nd,
Sr and Pb isotopic compositions of basal material, Earth Planet. Sci. Lett., 150, 161–169, 1997.

30 Wickert, A. D.: Reconstruction of North American drainage basins and river discharge since the Last Glacial Maximum, Earth Surf. Dynam.,
4, 831–869, https://doi.org/10.5194/esurf-4-831-2016, 2016.

Wilson, D. J., Piotrowski, A. M., Galy, A., and Clegg, J. A.: Reactivity of neodymium carriers in deep sea sediments: Implications for
boundary exchange and paleoceanography, Geochim. Cosmochim. Acta, 109, 197–221, 2013.

Winkler, A., Wolf-Welling, T. C. W., Stattegger, K., and Thiede, J.: Clay mineral seimentation in high northern latitude deep-sea basins since
35 the Middle Miocene (ODP Leg 151, NAAG), Int. J. Earth Sci., 91, 133–148, 2002.

Wooden, J. L., Czamanske, G. K., Fedorenko, V. A., Arndt, N. T., Chauvel, C., Bouse, R. M., King, B.-S. W., Knight, R. J., and Siems, D. F.:
Isotopic and trace-element constraints on mantle and crustal contributions to Siberian continental flood basalts, Noril'sk area, Siberia,
Geochim. Cosmochim. Acta, 57, 3677–3704, 1993.

Ziaja, W. and Pipała: Glacial recession 2001-2006 and its landscape effects in the Lindströmfjellet-Håbergnuten mountain ridge, Norden-
    skiöld Land, Spitsbergen, Pol. Polar Res., 28, 237–247, 2007.
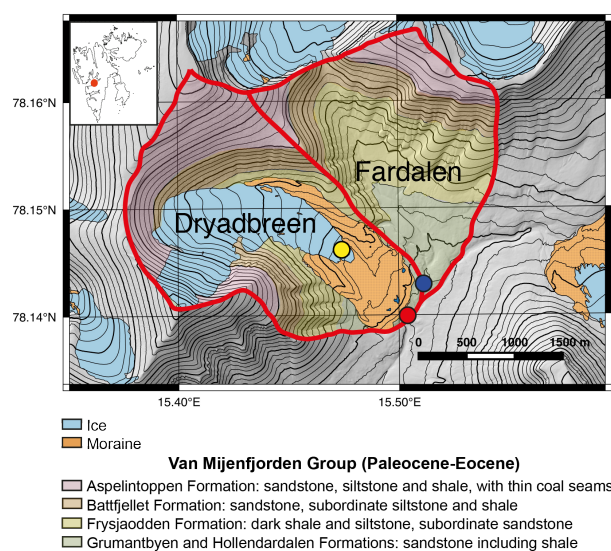
Figure 1. Topographic map of the sediment sampling locations with the geology of the catchments superimposed. Glaciers and their moraines are shown in blue and orange respectively and contours are displayed at 50 m intervals. The red dashed lines demarcate the catchment boundaries. Dryadbreen is on the left and Fardalen on the right. The coloured circles indicate where suspended sediment samples were collected; supraglacial sediment (yellow circle), Fardalen (blue circle) and Dryadbreen (red circle). Other rock and sediment samples were collected at various locations within the two catchments (Table 2). The red dot in the inset shows the location of the study area (Latitude, 78°08'N; Longitude, 15°30'E) in relation to the rest of Svalbard. Geological information is taken from (Major et al., 2000) and the topographic information is based on GIS data from the Norwegian Polar Institute.
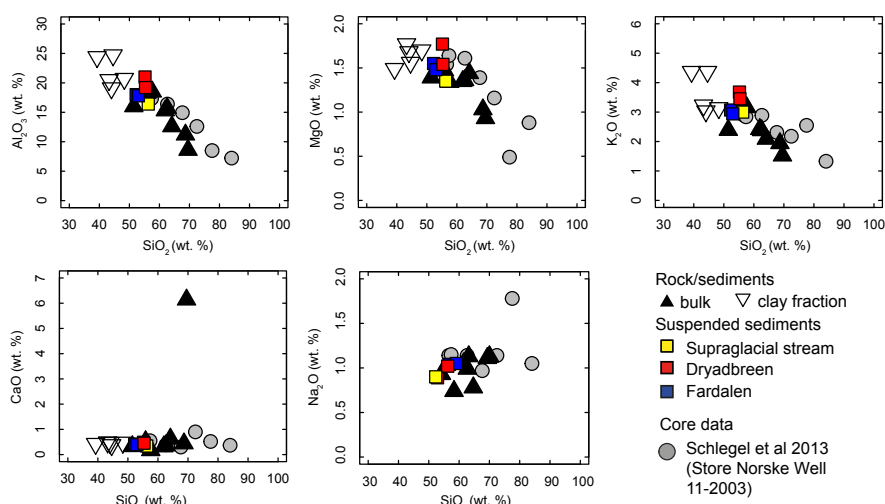
Figure 2. Plots of major elements against weight percent of SiO₂ compared with core data covering the same formations (Schlegel et al., 2013). Na concentrations in the clay-sized fraction are not plotted due the use of sodium phosphate in the clay separation method.
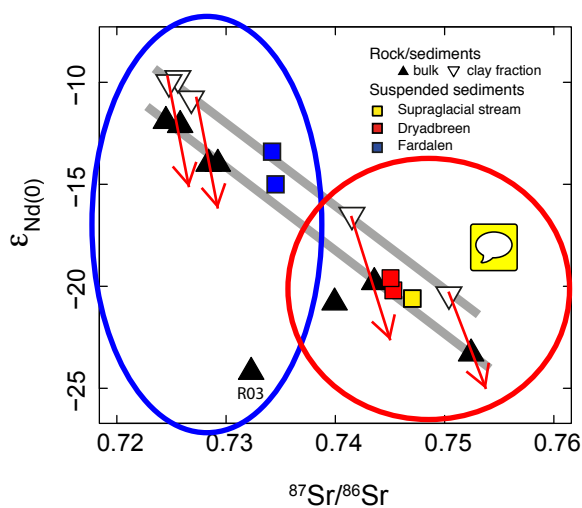
Figure 3. A plot of ^{87}Sr/^{86}Sr vs εNd$_0$. The grey lines highlight the parallel trends of the bulk and the clay-sized fraction data. Sample R03 is a litharenite whereas the other samples are predominantly shale (Table 1).
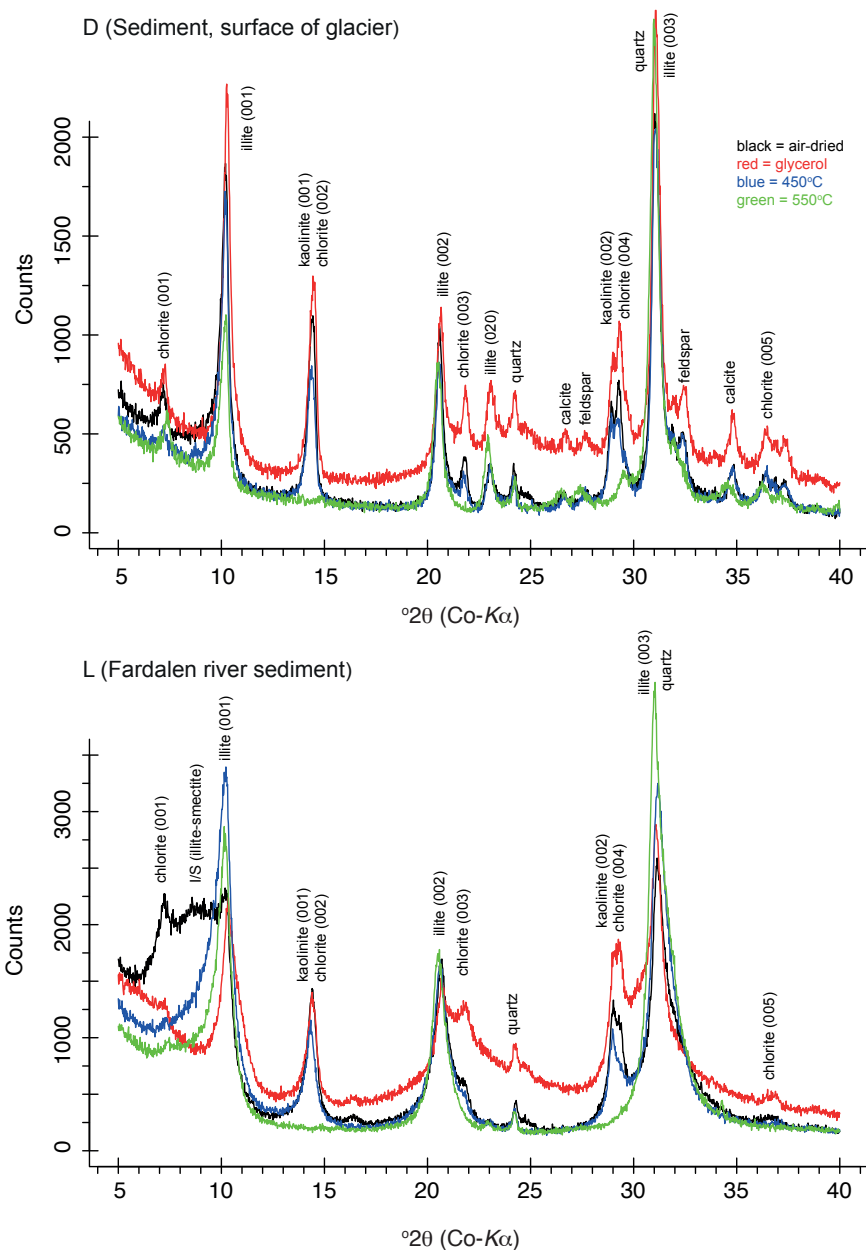
Figure 4. XRD patterns from two different samples: one with a high relative illite abundance (D) and one with low relative illite abundance and the clear presence of an expandable clay, likely an illite-smectite (I/S) mixed phase mineral (L).
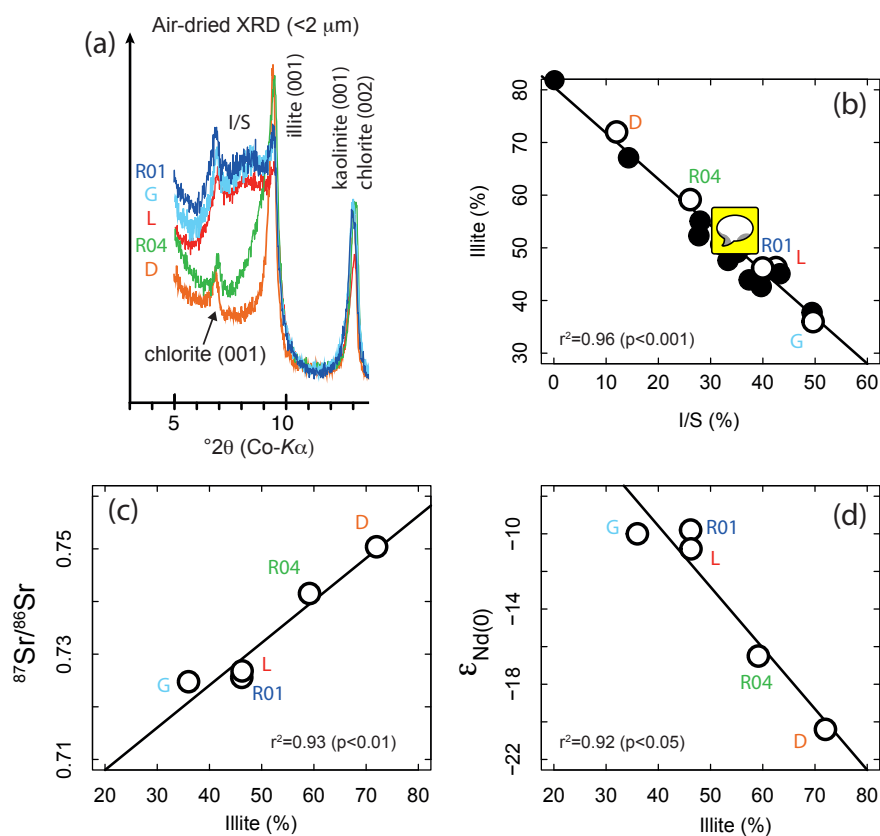
Figure 5. a Part of the orientated clay XRD spectrum (air-dried) for five samples. I/S stands for a mixed layer clay containing smectite and illite. Note the decrease in the I/S peak from R01 to D. **b** The relative abundances of illite and I/S in the clay fraction are inversely correlated **c,d** There is a positive correlation between the relative abundance of illite and the radiogenic strontium isotope ratio in the clay fraction and an inverse correlation with the radiogenic neodymium isotope ratio.
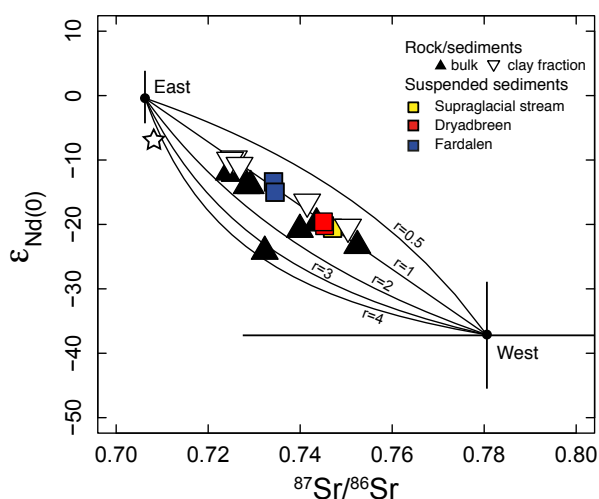
Figure 6. Plot of εNd_0 vs $^{87}Sr/^{86}Sr$. The two points 'East' and 'West' are averages of the interquartile range of literature data and the error bars indicate the interquartile range (for the 'East' source the error in $^{87}Sr/^{86}Sr$ is too small to see). 'East' data (n=99): Siberian Traps (Lightfoot et al., 1993; Wooden et al., 1993) and Uralides (Spadea and D'Antonio, 2006). 'West' data (n=65): Archaean rocks (predominantly gneisses, Jacobsen, 1988; Collerson et al., 1989; Kalsbeek and Frei, 2006; Friend et al., 2009), basal ice particles from GISP 2 and GRIP and granite bedrock samples from GISP 2 (Weis et al., 1997). The 'r' values are the Sr/Nd ratio of the 'East' source divided by the Sr/Nd ratio of the 'West' source. The star indicates the isotopic composition of Eocene seawater (see text for details, Gleason et al., 2009).

Earth **Surface**
Dynamics
Discussions
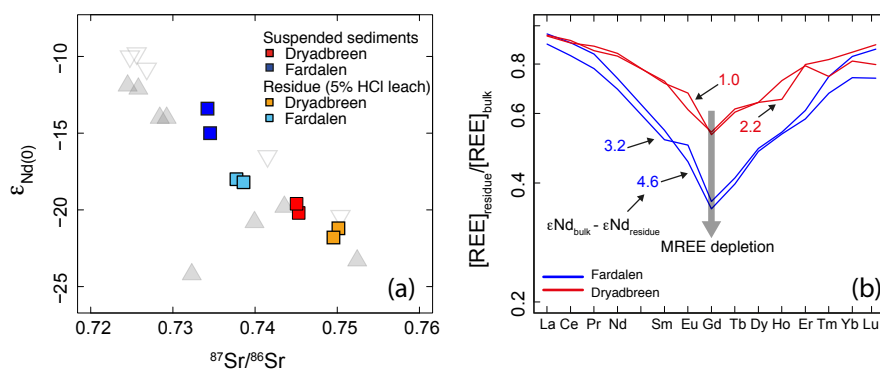
Figure 7. (**a**) εNd_0 and $^{87}Sr/^{86}Sr$ data for bulk suspended sediments and the residual solids after leaching with 5% HCl. In the background is the data from Fig. 3. (**b**) Rare earth element (REE) abundances of the residue relative to the bulk phase. The greater the depletion in middle REE (MREE), the greater the difference in εNd_0 between bulk and residual phases and this difference is most pronounced in the unglaciated catchment (Fardalen) where relative I/S abundances are higher compared to the glaciated catchment (Dryadbreen, Table 2). The residual phases has a lower εNd_0 value compared to the bulk.

Earth **Surface**
Dynamics
Discussions
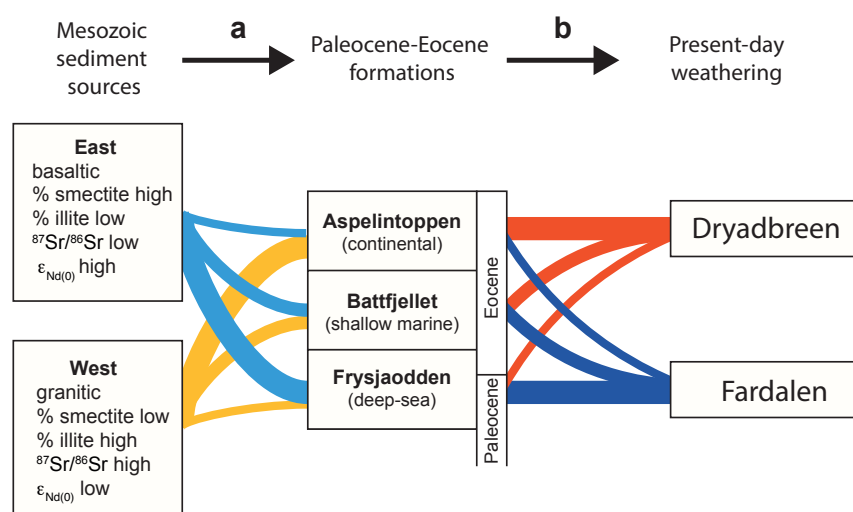
Figure 8. Summary of the processes leading to the variation in clay mineralogy, $^{87}Sr/^{86}Sr$ and εNd_0 observed in the two studied catchments. The thickness of the lines gives an indication of the relative contribution of Mesozoic sources to Eocene formations and the Eocene formations to suspended sediment export from the two catchments. For example, the Frysjaodden Formation receives a greater proportion of sediment from the eastern source as compared to the western source. (**a**) The contribution of Meoszoic sediment sources to Eocene formations is determined by the depositional location (far-shore vs near-shore), particle size and susceptibility to authigenic phase formation. (**b**) The contribution of the Paleogene formations to the present-day suspended sediment load is determined by the present-day exposure of the formations in each catchment (Fig. 1) which is determined by the recent erosional history of the catchments.

Earth **Surface Dynamics**
Discussions

Table 1. Major and selected trace metal concentrations, $^{87}Sr/^{86}Sr$ and εNd_0 values for solid samples. Major elements (in wt%) were measured by ICP-OES and trace elements (mg/kg) were measured by ICP-MS. REE data are presented in Table A2.

Name and description	SiO$_2$[1] wt%	Al$_2$O$_3$ wt%	Fe$_2$O$_3$ wt%	TiO$_2$ wt%	MgO wt%	CaO wt%	Na$_2$O wt%	K$_2$O wt%	LOI wt%	Mn mg/kg	Ba mg/kg	Sr mg/kg	Rb mg/kg	Nd mg/kg	Sm mg/kg	$^{87}Sr/^{86}Sr$	εNd_0
Bulk rock and sediment samples																	
R01 = shale (pieces)	63.2	15.7	7.07	0.79	1.36	0.36	1.13	2.38	7.9	497	438	98	103	32	6	0.724490	-11.9
R02 = wacke	64.7	12.6	7.99	0.56	1.44	0.63	0.78	2.09	8.9	1056	371	83	89	26	5	0.729241	-14.0
R03 = litharenite	70.0	8.6	3.26	0.56	0.93	6.14	1.13	1.52	7.7	480	366	139	54	25	5	0.732295	-24.2
R04 = shale (rock)	58.3	18.5	3.50	0.88	1.34	0.17	0.74	3.16	13.3	190	542	107	147	39	7	0.743564	-19.8
D = sediment (surface of glacier)	54.2	18.3	6.71	0.75	1.47	0.53	0.93	3.28	13.8	735	706	99	135	36	6	0.752425	-23.3
G = shale (pieces)	61.5	16.0	7.70	0.78	1.39	0.33	1.05	2.39	8.6	613	425	100	103	32	6	0.725796	-12.1
L = stream sediment (Fardalen)	62.7	15.3	7.68	0.74	1.35	0.32	0.99	2.42	8.2	692	448	99	104	32	6	0.728400	-1
O = stream sediment (Dryadbreen)	69.3	11.2	5.09	0.69	1.03	0.44	1.11	1.94	9.0	568	448	78	76	33	6	0.739930	-20.8
<2 μm fraction of bulk rock and sediment samples																	
R01-clay	49.6	20.7	9.26	0.65	1.70	0.48	2.08	3.14	9.6	452	451	82	142	38	8	0.725590	-9.8
R04-clay	53.6	24.7	3.63	0.72	1.56	0.38	3.45	4.37	11.9	163	664	132	200	32	6	0.741518	-16.5
D-clay	57.6	24.4	6.30	0.64	1.49	0.43	4.45	4.37	11.8	526	828	120	186	26	5	0.750395	-20.4
G-clay	52.0	19.1	8.82	0.60	1.68	0.47	4.04	3.03	10.1	650	427	93	132	33	6	0.724766	-10.0
L-clay	54.5	20.5	9.72	0.56	1.77	0.49	3.22	3.23	12.0	705	431	89	140	29	6	0.726819	-10.8
Suspended sediments (Bulk)[2]																	
20120801SG	47.7	16.4	5.72	0.74	1.35	0.34	0.90	3.00	19.1	482	687	98	123	34	6	0.747044	-20.6
20120617D	43.8	19.2	6.51	0.75	1.54	0.45	1.02	3.45	10.7	660	1031	105	142	34	6	0.745052	-19.6
20120618F	40.9	17.8	6.94	0.77	1.48	0.39	1.05	2.94	9.4	1227	738	108	128	40	8	0.734528	-15.0
20120726F	43.2	18.0	7.04	0.76	1.55	0.42	1.04	3.07	11.1	769	595	115	130	42	9	0.734207	-13.4
20120729D	47.1	21.0	7.37	0.82	1.77	0.49	0.89	3.68	10.9	660	756	114	162	37	7	0.745309	-20.2
Suspended sediments (Acid-treated)																	
20120617D(HCl)	43.9	20.2	6.44	0.73	1.45	0.06	1.04	3.56	10.3	366	1019	96	153	29	4	0.749536	-21.8
20120618F(HCl)	39.5	18.1	6.40	0.81	1.38	0.20	1.03	3.08	8.4	331	576	98	131	28	4	0.738594	-18.2
20120726F(HCl)	42.7	19.2	6.79	0.83	1.49	0.04	0.89	3.28	10.1	318	554	110	142	31	5	0.737735	-18.0
20120729D(HCl)	46.3	21.4	6.75	0.85	1.61	0.03	0.89	3.76	10.9	383	675	100	166	32	5	0.750142	-21.2

[1] SiO$_2$ concentrations calculated by assuming 100% recovery. For a comparison of XRF and ICP-OES concentrations see Table A1

[2] Samples names are YYYYMMDD and the subsequent letters are D=Dryadbreen (glaciated), F= Fardalen (unglaciated) and SG = supraglacial

Earth **Surface**
Dynamics
Discussions

Table 2. Relative proportions of clay minerals as determined from XRD patterns for the solid samples collected in the two catchments. Samples are ordered from highest to lowest relative illite abundance.

Sample	Description	Catchment[1]	Illite (%)	I/S (%)	Kaolinite (%)	Chlorite (%)
I	fossil-rich rock	D	82	0	9	9
D	sediment (surface of glacier)	D	72	12	7	9
R03	sandstone	D	67	14	8	10
R04	shale (rock)	D	59	26	7	7
A	sandur sediment	D	52	28	8	12
F	moraine sediment	D	55	28	8	9
O	stream sediment	D	51	32	8	9
R02	siltstone	D	48	33	5	14
H	soil	F	49	35	9	7
M	stream bank sediment	F	51	37	6	7
C	moraine sediment	D	44	37	9	10
E	shale rock	D	43	40	8	9
R01	shale (pieces)	F	46	40	7	7
N	stream bedload	F	46	41	6	7
L	stream sediment	F	46	43	5	6
K	stream sediment	F	45	43	6	6
B	shale (pieces)	D	38	49	6	7
G	shale (pieces)	F	36	50	7	7

[1] Catchment where sample was collected. F=Fardalen, D= Dryadbreen.

[2] I/S is an illite-smectite mixed phase mineral.

Appendix A

Table A1. Comparison of element concentrations collected by XRF (only available for four samples) and ICP-OES. Data from ICP-OES is used in the paper.

Name and description	SiO_2[1] wt%	Al_2O_3 wt%	Fe_2O_3 wt%	TiO_2 wt%	MgO wt%	CaO wt%	Na_2O wt%	K_2O wt%	P_2O_5 wt%	LOI wt%	Sum wt%	Mn mg/kg	Ba mg/kg	Sr mg/kg	Rb mg/kg	Nd mg/kg	Sm mg/kg
Data collected by XRF																	
R01	63.2	16.3	7.1	0.8	1.4	0.3	1.0	2.6	0.3	7.5	100.5	488	403	97.4	102	35	<10
R02	65.4	13.0	7.9	0.6	1.5	0.6	0.7	2.2	0.3	7.2	99.4	1038	357	81.9	88.8	27	<10
R03	70.9	8.9	3.2	0.6	0.9	6.2	1.1	1.6	0.1	7.0	100.5	472	356	142	55.1	23	<10
R04	57.1	19.1	3.5	0.9	1.3	0.2	0.6	3.6	0.1	12.9	99.3	178	511	116	150	42	<10
Data collected by ICP-OES[1]																	
R01	63.2	15.7	7.1	0.8	1.4	0.4	1.1	2.4	0.2	7.9	100.0	497	438	98	103	32	6
R02	64.7	12.6	8.0	0.6	1.4	0.6	0.8	2.1	0.3	8.9	100.0	1056	371	83	89	26	5
R03	70.0	8.6	3.3	0.6	0.9	6.1	1.1	1.5	0.1	7.7	100.0	480	366	139	54	25	5
R04	58.3	18.5	3.5	0.9	1.3	0.2	0.7	3.2	0.1	13.3	100.0	190	542	107	147	39	7

[1] SiO_2 concentrations calculated by assuming 100% recovery.

Earth **Surface** Dynamics Discussions EGU Open Access

Table A2. Rare earth element concentrations in mg/kg[1].

Sample[2]	La	Ce	Pr	Nd	Sm	Eu	Gd	Tb	Dy	Ho	Er	Tm	Yb	Lu
Bulk rock and sediment samples														
R01	35.7	71.2	8.4	32.4	6.0	1.2	4.5	0.7	4.0	0.7	2.0	0.3	1.9	0.3
R02	28.5	55.5	6.6	25.7	4.8	1.1	3.8	0.6	3.2	0.6	1.7	0.2	1.5	0.2
R03	30.5	60.3	6.8	25.4	4.5	0.9	3.1	0.4	2.2	0.4	1.0	0.1	0.9	0.1
R04	49.1	95.4	10.7	39.3	6.6	1.3	4.0	0.7	3.5	0.7	1.9	0.3	1.8	0.2
D	43.9	88.5	9.9	36.5	6.5	1.2	4.3	0.6	3.3	0.6	1.6	0.2	1.4	0.2
G	35.7	70.4	8.3	32.3	6.0	1.3	4.6	0.7	4.2	0.8	2.3	0.3	2.2	0.3
L	37.1	72.8	8.3	31.6	5.8	1.2	4.4	0.7	4.0	0.8	2.2	0.3	2.0	0.3
O	37.9	76.3	8.7	33.4	5.9	1.1	4.2	0.6	3.1	0.5	1.4	0.2	1.3	0.2
<2 μm fraction fraction of bulk rock and sediment samples														
R01-clay	37.0	72.7	9.4	38.1	8.0	1.8	7.1	1.0	5.8	1.0	2.8	0.4	2.5	0.3
R04-clay	38.9	78.0	8.6	31.9	5.8	1.0	3.7	0.6	3.5	0.7	2.0	0.3	2.0	0.3
G-clay	32.4	64.3	8.0	32.6	6.5	1.5	5.7	0.9	4.8	0.9	2.4	0.3	2.2	0.3
D-clay	31.5	64.0	7.0	25.9	4.8	1.0	3.8	0.6	3.4	0.7	1.8	0.3	1.7	0.2
L-clay	30.5	60.4	7.1	29.0	6.0	1.4	5.4	0.9	4.9	1.0	2.7	0.4	2.5	0.4
Suspended sediments (Bulk)[2]														
20120801SG	41.8	82.8	9.4	34.4	6.2	1.2	4.2	0.6	3.3	0.6	1.6	0.2	1.5	0.2
20120617D	40.3	79.3	9.1	34.1	6.2	1.2	4.3	0.6	3.5	0.6	1.6	0.2	1.5	0.2
20120618F	40.9	84.5	10.0	40.3	8.2	1.8	7.1	1.0	5.4	1.0	2.5	0.3	2.0	0.3
20120726F	44.3	89.6	10.4	41.8	8.6	1.9	7.7	1.2	6.3	1.1	2.9	0.4	2.4	0.3
20120729D	44.6	88.9	9.9	37.3	6.6	1.3	4.7	0.7	3.7	0.7	1.8	0.3	1.7	0.3
Suspended sediments (Acid-treated)														
20120617D(HCl)	38.1	72.8	7.9	28.6	4.5	0.7	2.3	0.4	2.2	0.4	1.3	0.2	1.3	0.2
20120618F(HCl)	36.8	71.0	7.8	27.8	4.2	0.9	2.5	0.4	2.7	0.5	1.5	0.2	1.7	0.2
20120726F(HCl)	42.2	81.2	8.8	30.7	4.7	0.9	2.7	0.5	3.0	0.6	1.7	0.3	1.8	0.2
20120729D(HCl)	42.1	80.4	8.8	31.7	4.7	0.9	2.5	0.4	2.4	0.5	1.4	0.2	1.4	0.2

[1] The hotplate digestion method used does not digest zircons and therefore the high rare earth element (HREE) concentrations may be lower than the true total. Nd and Sm are fully digested by the hotplate method (Rickli et al., 2013).

[2] Please refer to Table 1 for sample descriptions.